Desalination and Water Treatment
www.deswater.com
doi: 10.1080/19443994.2014.883333

54 (2015) 511–524
April

Taylor & Francis
Taylor & Francis Group

Adsorption behavior of Cr(VI), Ni(II), and Co(II) onto zeolite 13x

Yanping Jin[a], Yunhai Wu[a], Julin Cao[b], Yunying Wu[c,*]

[a]*Key Laboratory of Integrated Regulation and Resources Development of Shallow Lakes, Ministry of Education, Hohai University, Nanjing, China*
[b]*College of Environment, Hohai University, Nanjing 210098, China*
[c]*Department of Chemistry, Hanshan Normal University, Chaozhou, China*
Tel./Fax: +86 768 2318681; email: jinyanping0408@aliyun.com

Received 21 August 2013; Accepted 4 January 2014

ABSTRACT

The adsorbed behavior of zeolite 13x was tested for the removal of chromium (Cr(VI)), nickel (Ni(II)), and cobalt (Co(II)) in single- and multi-solute (binary and ternary) systems, using a batch adsorption technique under different experimental conditions namely solution pH and initial metal-ion concentration. pH 6 was the optimum condition for the adsorption of Cr(VI), Ni(II), and Co(II). The removal rate decreased as the temperature and the initial concentration increased. Kinetics experiments indicated that the processes can be simulated by pseudo-second-order model. The Langmuir adsorption model fitted the experimental data reasonably well better than Freundlich, D–R, and Redlich–Peterson model for the three metal ions studied. The maximum monolayer adsorption capacity for Cr(VI), Ni(II), and Co(II) was 3.929, 6.195, and 10.389 mg/g, respectively. The main energy of adsorption (E), calculated as 8–16 kJ/mol, demonstrated chemical characteristics of adsorption process. Thermodynamic calculations showed that the adsorption of all metal ions onto zeolite 13x was feasible, endothermic in nature and the degrees of freedom increased at the solid–liquid interface during the adsorption. The sequential adsorption–desorption cycles showed that hydrochloric acid held good desorption on saturated zeolite.

Keywords: Adsorption; Desorption; Isotherm; Kinetics; Thermodynamics; Zeolite 13x

1. Introduction

The removal of heavy metal ions, such as chromium (Cr(VI)), nickel (Ni(II)), and cobalt (Co(II)) from industrial effluents has been attracting great attention because of their toxicity towards aquatic fauna, aquatic flora, and even human [1]. Conventional technologies for Cr(VI)), Ni(II), and Co(II) removal from wastewaters include chemical precipitation, membrane separation, electrolysis, ion exchange, and adsorption. Among these technologies, adsorption is found to be cheap, effective, and easy to adapt [2,3]. Many types of adsorbents have been used for the removal of Cr(VI), Ni(II), and Co(II), including: (1) biomass, such as Mucor hiemalis [4], *Schizosaccharomyces pombe* [5], chitosan [6], rice husk [7], red pine sawdust [8], almond green hull [9], *Sargassum wightii* [10], and activated carbon [11]; (2) clay mineral materials such as zeolite [12], clinoptilolite [13], Bofe bentonite clay [14], Al-pillared bentonite clay [15], and hydroxyapatite [16]; and (3) other materials such as poly [17], silica gel [18], and chelating resins [19]. There are many

*Corresponding author.

reports available for the adsorption of heavy metals by zeolite 13x [20,21].

Zeolite 13x [22] is recognized to be an excellent sorbent for its high ion exchange capacity, selectivity, and compatibility with the natural environment. Besides, they are microporous crystalline aluminosilicates and their framework exhibits negative charge because of the isomorphous substitution of Al^{3+} for Si^{4+} [23]. These negative charges appear on the AlO_4^- groups of the framework and are compensated by extra framework cations or through the interaction of framework oxygen atoms and protons with the formation of acid hydroxyls [24]. It is easy to find out that zeolite 13x could be an excellent potential adsorbent.

The objective of the present study is to investigate the feasibility of using zeolite 13x as an adsorbent for the individual and simultaneous removal of Cr(VI), Ni(II), and Co(II) from aqueous solutions, to present the experimental equilibrium sorption data, and to examine the applicability of various multi-component adsorption isotherm equations to the competitive adsorption equilibrium of the metal ions (Cr(VI), Ni(II), and Co(II)) in binary and ternary system. Also, the mechanism involved in the removal of these metal ions onto the zeolite 13x was studied in detail and desorption was also carried out for better understanding of the removal process.

2. Experimental methods

2.1. Materials

The zeolite 13x with $\gamma_{Al:Si} = 5.36$ used in this work was from China National Medicine Corporation Ltd, Shanghai, China. The main physical characteristics of zeolite 13x, such as mean pore radius (3.02 nm), BET surface area (621 m^2/g), and total pore volume (0.94 cm^3/g) were given by the company. And the zeolite 13x particles were ground to pass a 60-mesh sieve (0.42 mm), and then dried at 105°C for 24 h in the oven, leached into a dry dish for further use. All the other reagents used in this work were of analytical grade. Stock solutions of 1,000 mg/L were prepared by dissolving appropriate amounts of Cr(VI), Ni(II), and Co(II) nitrate salts in distilled water. Working solutions were prepared by suitable dilution of the stock solutions. Adjustment of pH was carried out using 0.1 M NaOH or 0.1 M HCl.

2.2. Methods

Cr(VI), Ni(II), and Co(II) concentrations were determined by the diphenylcarbazide [25], dimethylglyoxime [26], and 4-[(5-chloro-2-pyridyl) azo]-1,3-diaminobenzene (5-Cl-PADAB) [27] colorimetric method at a wavelength of 540, 530, and 570 nm using a UV–vis spectrophotometer (Ruili Analytical Instrument Corporation Ltd, Beijing, China), respectively.

The X-ray diffraction (XRD) (ARL Corp, Switzerland) patterns were acquired on a diffractometer operated at 40 kV and 40 mA with Cu radiation and the diffraction measurements were conducted within the 2θ angle of 3–50°, at the scanning rate of 5°/min.

2.3. Batch operations

Single, binary, and ternary adsorption of Cr(VI), Ni(II), and Co(II) onto zeolite 13x were performed in a batch mode at 313 K. Basically, 0.5 g of zeolite 13x was added to 100 mL of solute concentration, at the desired pH, in 250 mL Erlenmeyer flasks and was agitated at 130 rpm in a shaking thermostat machine (SHA-BA type) for 4 h. The contact time and conditions were selected on the basis of preliminary experiments, which demonstrated the equilibrium was established in 360 min. All equilibrium tests were conducted for 360 min. At the end of the experiment, the content of the flask was separated by filtration. The effect of pH on the removal of zeolite 13x was evaluated by adjusting the pH in the range of 1–8 for Cr(VI) and Co(II), 1–7 for Ni(II) with the concentration of 5, 20, and 25 mg/L, respectively. Adsorption kinetics studies were carried out at pH 6, predetermined initial metal concentration, and the samples were withdrawn at predetermined time intervals. For isotherm experiments, the initial metal concentration varied from 0 to 100 mg/L for each metal ion in single, binary, and ternary systems. The experiments were carried out at different temperature (298–313 K). The removal ratio (R (%)) and the adsorption capacity at equilibrium (q_e (mg/g)) of Cr(VI), Ni(II), and Co(II) can be calculated using the following equations:

$$R(\%) = \frac{(C_0 - C_e)}{C_0} \times 100 \quad (1)$$

$$q_e = \frac{(C_0 - C_e)V}{M} \quad (2)$$

All the batch experiments were conducted in duplicate, and the average values were reported. The relative errors of data were about 5%.

2.4. Desorption study

For the adsorption–desorption studies, 1.0 g of zeolite 13x was added to 100 mL of 10 mg/L Cr(VI), 50

mg/L Ni (II), and 50 mg/L Co(II) ion solution, shaken at pH 6 and kept in 250 mL Erlenmeyer flasks. The Cr(VI)–Ni(II)–Co(II)–zeolite 13x complex was collected by filtration and washed several times with distilled water to remove any unabsorbed metal ions and oven dried at 313 K. The amount of Cr(VI), Ni(II), and Co(II) adsorbed per gram of zeolite 13x was determined from the metal ion concentration remaining in each solution. Then, 0.1 M $CaCl_2$, 0.1 M NaOH, 0.1 M NaCl, 0.1 M HCl, and distilled water solutions were used as desorbing agents. The amount of metal ions desorbed was then measured by the percentage of desorption that was calculated from the following expression:

$$\text{Desorption}(\%) = \frac{\text{Amount of metal ions desorbed}}{\text{Amount of metal ions adsorbed}} \times 100 \quad (3)$$

All chemicals used in the experiments were purchased in analytical purity and used without any purification. All solutions were prepared with deionized water.

3. Results and discussion

3.1. Effect of pH for single-ion situation

One of the most critical parameters in the adsorption process of metal ions from aqueous solutions is the pH of the medium. Fig. 1 shows the effect of solution pH on the equilibrium removal efficiency of Cr(VI), Ni(II), and Co(II) ions. The pH range for the adsorption study was chosen so as the formation of nickel hydroxide precipitation may occur above pH 8. Fig. 1 indicates that the removal of Cr(VI) increased with increasing pH from 1 to 6 and then decreased as pH rise from 6 to 8. Similar trends were also observed for cobalt removal. And Ni(II) adsorption increases with the increase of pH. These observations suggest that H^+ ions should be considered as competitive ones in the adsorption processes [28]. At low pH values, the concentration of H_3O^+ far exceeds that of the metal ions, hence these H_3O^+ are mainly bound to the adsorbent, leaving the large number of metal ions unbound. When the pH is increased, the concentration of hydronium ions decreases and the positively charged metal ions adsorbed on the free binding sites. The pH effect may be the competition effect between the hydronium ions and metal ions, because when metal ions associate with adsorbent, they have to compete with the hydronium ions for the active sites on the surface of the adsorbent. The working pH for adsorption was determined as 6 for Cr(VI), Ni(II), and Co(II). Similar results appeared in previous studies related to the adsorption of Cr(VI), Ni(II), and Co(II) on poly (aryl ether ketone) containing pendant carboxyl groups (PEK-L) [17] and calcined Bofe bentonite clay [14].

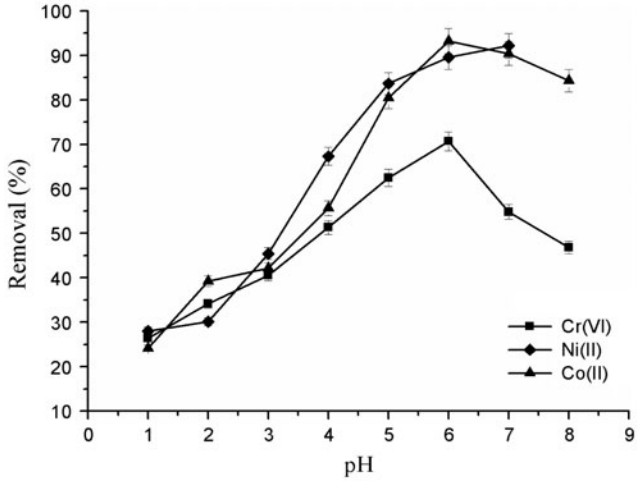

Fig. 1. Effect of pH on the adsorption of metal ions onto zeolite 13x in the single-ion situation (initial concentration of Cr(VI) = 5 mg/L, Ni(II) = 20 mg/L and Co(II) = 25 mg/L; contact time = 4h; shaking rate = 130 rpm; and adsorbent dosage = 0.5 g).

3.2. The competitive adsorption of ions from binary system

The competitive adsorption for Cr(VI)–Ni(II), Cr(VI)–Co(II), and Ni(II)–Co(II) binary solutes were obtained by fixing the initial concentration of interferential metal ions. It is clear from Fig. 2 that the removal rate decreases with increasing concentration. These results may be explained that the initial metal concentration provides a driving force to overcome all mass transfer resistances between the sorbent and sorption medium. Hence, higher sorption capacities were obtained at a higher initial metal concentration of the three metal ions.

As shown in Fig. 2(b) and (c), the presence of Co(II) ion resulted in the inhibition in Cr(VI), Ni(II), and Co(II) uptake, and this observation was much more significant than those in the presence of Cr(VI) – Ni(II) system (Fig. 2(a)). The removal rate of the binary and ternary metal mixture was lower than that of noncompetitive conditions. The results clearly showed that the combined action of multiple ions was antagonistic. The most likely reason for the antagonistic effect was the competition for adsorption sites on the surfaces and/or the screening effect of the competing metal ions. The results also confirmed that Co(II) exerted the inhibitoriest effect on the adsorption of other metals, followed by Ni(II) and Cr(VI).

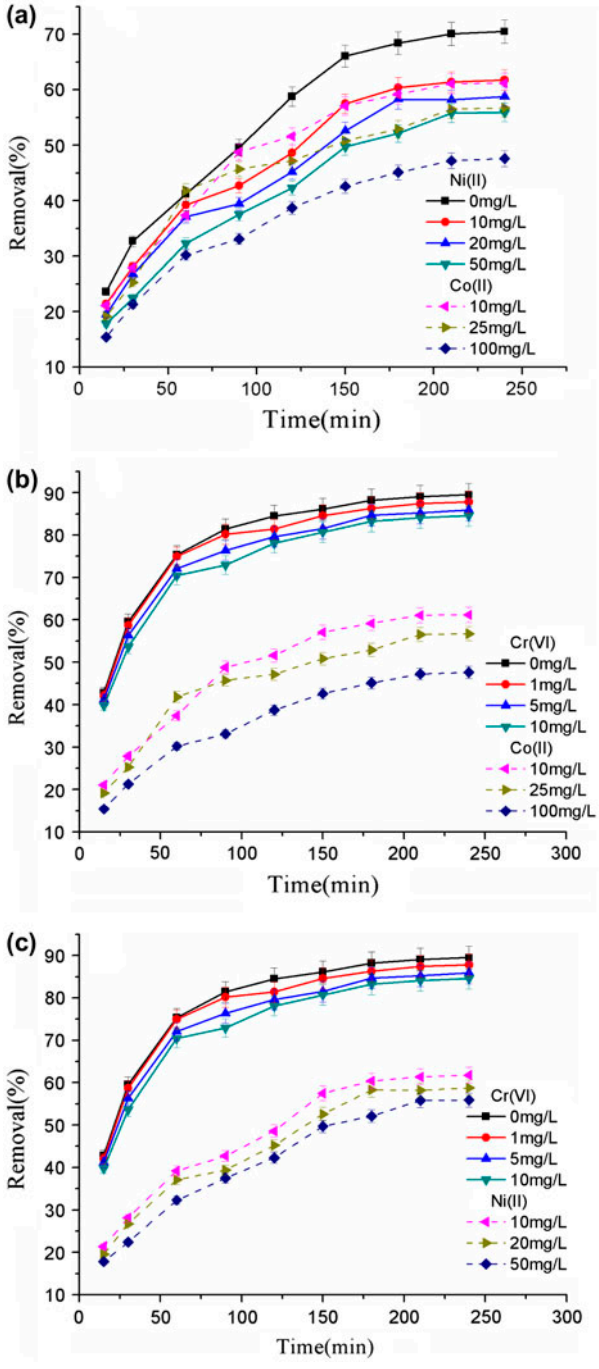

Fig. 2. (a) Time profiles of Cr(VI) adsorption by zeolite 13x in mixture of Cr–Ni or Cr–Co at different concentrations (initial concentration of Cr(VI) = 5 mg/L; pH = 6; shaking rate = 130 rpm; adsorbent dosage = 0.5 g). (b) Time profiles of Ni(II) adsorption by zeolite 13x in mixture of Ni–Cr or Ni–Co at different concentrations (initial concentration of Ni(II) = 20 mg/L; pH = 6; shaking rate = 130 rpm; adsorbent dosage = 0.5 g). (c) Time profiles of Co(II) adsorption by zeolite 13x in mixture of Co–Cr or Co–Ni at different concentrations (initial concentration of Co(II) = 25 mg/L; pH = 6; shaking rate = 130 rpm; adsorbent dosage = 0.5 g).

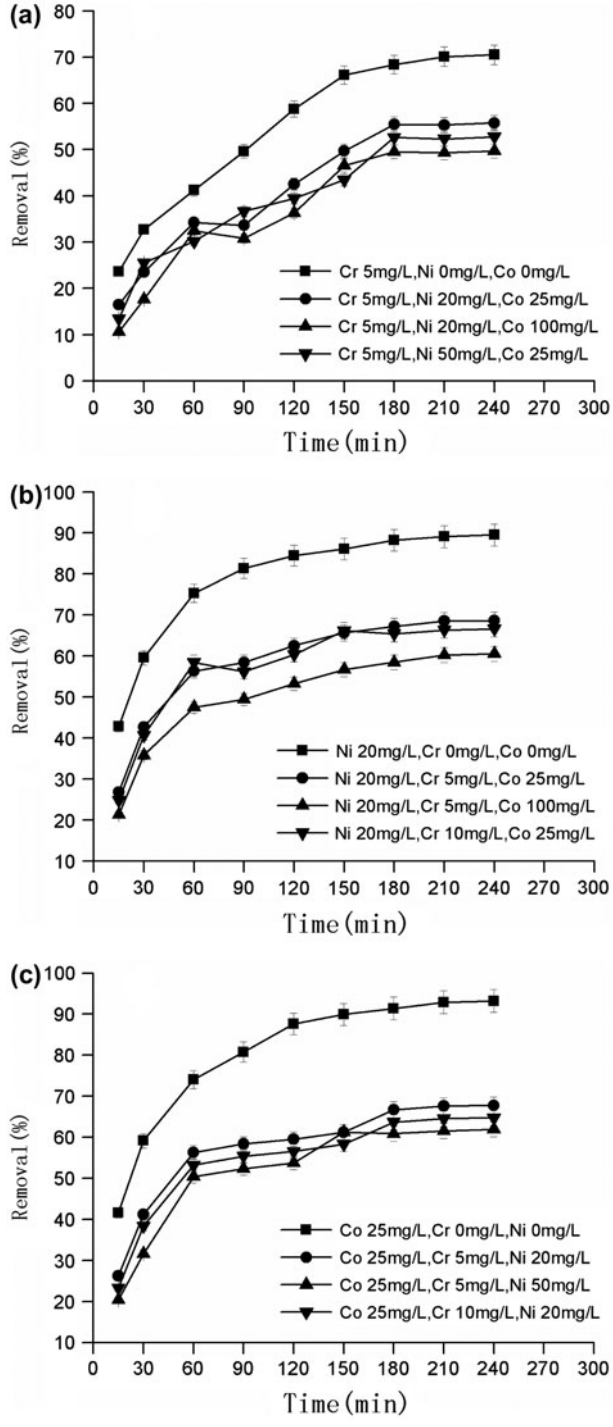

Fig. 3. Time profiles of metal sorption by zeolite 13x in mixture of Cr(VI), Ni(II) and Co(II) at different concentration: (a) Cr(VI); (b) Ni(II); and (c) Co(II) (pH = 6; shaking rate = 130rpm; adsorbent dosage = 0.5 g).

A similar phenomenon had been observed in the binary adsorption Ni(II) and Co(II) adsorption onto EDTA- and/or DTPA-modified chitosan [6], where it was shown that the modified chitosan had a much better affinity for Ni(II) than for Co(II) suggesting that Ni(II) could be adsorbed selectively from the contaminated water in the presence of Co(II).

3.3. The competitive adsorption of ions from ternary system

The tri-metal adsorption of Cr(VI), Ni(II), and Co(II) by zeolite 13x was investigated to establish the effect of the presence of two metal ions on the adsorption of each one of them. The equilibrium removal of any ion by zeolite 13x in the presence of varied concentration of other ions as function of metal concentration and contact time was compared with those in the single-ion situation (Fig. 3). As shown in Fig. 3(a), the highest removal of Cr(VI) was found to be 70.71% in the single-ion situation, while the lowest removal obtained in the ternary metal solutions at the same initial concentration of Cr(VI) and adsorption conditions, was found to be 49.68%. The presence of Ni(II) and Co(II) in solution showed no significant influence on the capacity of Cr(VI) adsorption on zeolite13x.

Fig. 3(b) shows that Ni(II) adsorption in single component system was better than in ternary system. The lowest removal of Ni(II) was found to be 60.54% was obtained in Cr(VI) (5 mg/L)–Ni(II) (20 mg/L)–Co(II) (100 mg/L) component system. It was lower than in Cr(VI) (5 mg/L)–Co(II) (25 mg/L) component system (68.65%), but higher than in Cr(VI) (10 mg/L)–Co(II) (25 mg/L) component system (66.65%).

Co(II) adsorption in single component system was also better than that of ternary component system (Fig. 3(c)). The highest removal of Co(II) was found to be 93.2%. It was higher than in Cr(VI) (5 mg/L)–Ni(II) (20 mg/L) component system (67.78%), Cr(VI) (5 mg/L)–Ni(II) (50 mg/L) component system (61.94%), and Cr(VI) (10 mg/L)–Ni(II) (20 mg/L) component system (64.78%).

Multi-component systems have additional features than. those of single components. According to the description above, the combined effect of the binary and ternary mixture seems to be antagonistic.

It is clear that the affinity of zeolite 13x for the studied ions varies as follows: Co(II) > Ni(II) > Cr(VI). The results can be explained by the physical and chemical properties of the metal ions—the ionic radii of metals [29]. This means that it is an important factor for ions exchanging in terms of the process of diffusion and sites of adsorption in the zeolite. Because of the atomic radii of Co(II) and Ni(II) are 0.082 and 0.078 nm, and hence these cations are easily exchanged with those of zeolite 13x (13.6 nm). Moreover, the Cr(VI) is usually present in liquid solutions in the form of chromate (CrO_4^{2-}) and dichromate ($Cr_2O_7^{2-}$), which are anions [30]. It is generally thought that zeolites which have anionic charge have little affinity for anionic metals [30,31]. The removal rate increased with increasing pH to a maximum value (pH 6) and then declined rather rapidly with further increase in pH. The decrease of removal rate at pH values greater than 6 is mainly due to hydroxide chromium species [32].

3.4. Adsorption kinetics study

The sorption of Cr(VI), Ni(II), and Co(II) from liquid to solid phase can be considered as a reversible reaction with equilibrium established between two phases. The specific rate constant of the sorption for sorbate and sorbent was determined from the pseudo-first-order rate and pseudo-second-order rate expressions.

Table 1
Kinetic parameters for adsorption of Cr(VI), Ni(II) and Co(II) by zeolite 13x at different temperatures

		Pseudo-first-order model			Pseudo-second-order model		
Metal ions	Temperature (K)	k_f	q_e	R^2	k_s	q_e	R^2
Cr(VI)	298	0.0198	0.619	0.9495	0.0213	0.7814	0.9887
	303	0.0191	0.660	0.9273	0.0232	0.8171	0.9882
	313	0.0201	0.708	0.9398	0.0252	0.8684	0.9854
Ni(II)	298	0.0237	3.350	0.9636	0.0108	3.7323	0.9996
	303	0.0221	3.452	0.9653	0.0124	3.7327	0.9996
	313	0.0221	3.601	0.9613	0.0147	3.8635	0.9999
Co(II)	298	0.0221	4.361	0.9899	0.0078	4.8665	0.9995
	303	0.0207	4.513	0.9758	0.0086	4.9481	0.9996
	313	0.0202	4.71	0.9673	0.0094	5.1199	0.9997

3.4.1. Pseudo-first-order kinetic model

The pseudo-first-order equation is [33]:

$$\log(q_e - q_t) = log\ q_e - \frac{k_f}{2.303}t \quad (4)$$

3.4.2. Pseudo-second-order kinetic model

The pseudo-second-order kinetic model is expressed as [33]:

$$\frac{t}{q_t} = \frac{1}{k_s q_e^2} + \frac{1}{q_e}t \quad (5)$$

For evaluating the adsorption kinetics of Cr(VI), Ni(II), and Co(II), the pseudo-first-order and pseudo-second-order models were used to fit the experimental data. The values of different parameters determined from different kinetic models for the three metal ions along with their correlation coefficient values (R^2) are presented in Table 1. The correlation coefficients for the second-order kinetic model are nearly equal to 1 and the theoretical values of q_e also agree very well with the experimental values. This suggests that the adsorption of Cr(VI), Ni(II), and Co(II) follows the second-order kinetic model better.

3.4.3. External diffusion model

In the present study, the Spahn and Schlünder model [34] was chosen to describe the external diffusion on the adsorbent:

$$\ln\frac{C_t}{C_0} = k_{ext}\left(\frac{A}{V}\right) \times t \quad (6)$$

If the Spahn and Schlünder model is applicable, the plot of $\ln\left(\frac{C_t}{C_0}\right)$ against time t should give a linear relationship.

The above theory considers kinetics governed by the rates of the surface reactions. Furthermore, to investigate whether film or pore diffusion was the controlling step in the adsorption, a model of intra-particle diffusion was tested as follows.

3.4.4. Intra-particle diffusion model

The intra-particle diffusion model is based on the theory proposed by Weber and Morris [35]. According to this theory:

$$q_t = k_{id}t^{\frac{1}{2}} + I \quad (7)$$

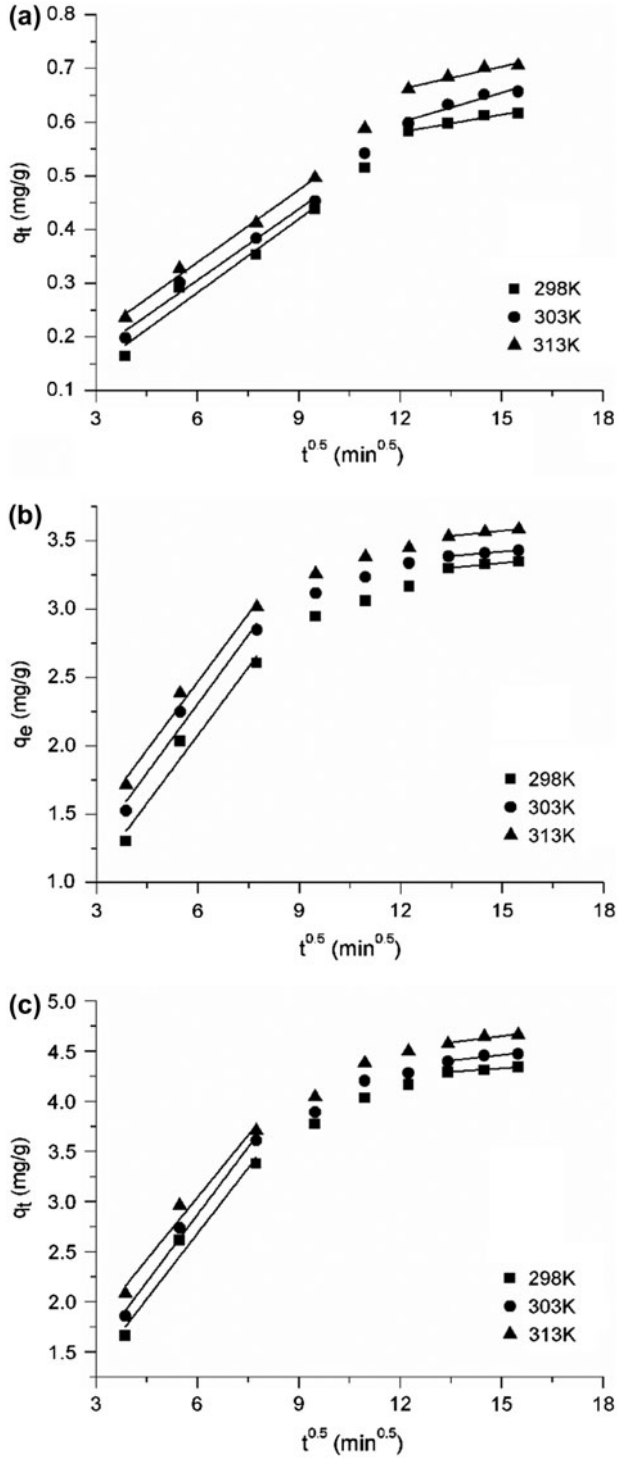

Fig. 4. Test of intra-particle diffusion model for adsorption Cr(VI), Ni(II) and Co(II) on to zeolite 13x (temperature 298, 303 and 313 K; the initial concentration of Cr(VI) (5 mg/L), Ni(II) (20 mg/L) and Co(II) (25 mg/L); shaking rate = 130rpm).

Fig. 4 presents the plots of Cr(VI), Ni(II), and Co(II) at different temperatures, q_t vs. $t^{1/2}$. The data exhibit a multilinear plot, indicating that more than one step influences the sorption process. The first sharp portion indicates the external surface sorption, while the second curved portion is the gradual sorption stage, where intra-particle diffusion is the rate-limiting step. This final linear portion is the equilibrium stage where sorption slows down due to an extremely low solute concentration. In the present study, the plots do not pass through the origin and have intercepts, I, a measure of the boundary layer thickness, i.e. the larger the value of intercept, the greater the boundary layer effect. The values of rate parameter, $k_{p.i}$ (i = stage number), calculated from the slope of the linear portion of the plot, which are listed in Table 2. As seen from the table, the order of adsorption rate was the second stage ($k_{p.2}$) > third stage ($k_{p.3}$) > k_{ext}. It has been reasonably concluded that the adsorption of the external surface reached saturation, and the metal ions entered into the pores within the particle and eventually were adsorbed on the active sites of the adsorbent internal surface. As the diffusion resistance increases with time, the diffusion rate decreases, thus, sorption is a multi-step process involving transport of metal ions to the surface of the sorbents followed by diffusion into the interior of the pores [36].

Table 2
The values of rate parameters of different stages for external diffusion and intra-particle diffusion equation (temperature 298, 303, and 313 K; the initial concentration of Cr(VI) (5 mg/L), Ni(II) (20 mg/L) and Co(II) (25 mg/L))

Metal ions	Temperature (K)	External diffusion	Intra-particle diffusion	
		k_{ext}	$k_{p.2}$ (mg g^{-1} min$^{-1/2}$)	$k_{p.3}$ (mg g^{-1} min$^{-1/2}$)
Cr(VI)	298	0.0048	0.0441	0.0109
	303	0.0049	0.0456	0.0139
	313	0.0053	0.0461	0.0183
Ni(II)	298	0.0153	0.3311	0.0232
	303	0.0166	0.3367	0.0243
	313	0.0183	0.3378	0.0252
Co(II)	298	0.0156	0.4358	0.024
	303	0.0177	0.4487	0.0364
	313	0.0179	0.4535	0.0437

Table 3
Kinetic parameters for Cr(VI), Ni(II) and Co(II) in binary system onto zeolite 13x

Binary system	Metal ions	Concentration (mg/L)	Pseudo-first-order			Pseudo-second-order		
			k_1	$q_{e,cal}$	R^2	k_2	$q_{e,cal}$	R^2
Cr–Ni	Cr	C_{Ni} = 10	0.0164	0.638	0.9657	0.0221	0.7535	0.9823
		C_{Ni} = 20	0.0162	0.622	0.9326	0.025	0.7217	0.9764
		C_{Ni} = 50	0.0154	0.578	0.9326	0.0254	0.7032	0.9781
	Ni	C_{Cr} = 1	0.0177	3.623	0.8132	0.015	3.7806	0.9997
		C_{Cr} = 5	0.0183	3.512	0.8879	0.0143	3.7094	0.9997
		C_{Cr} = 10	0.0212	3.416	0.9142	0.0131	3.6839	0.9996
Cr–Co	Cr	C_{Co} = 10	0.0179	0.622	0.9147	0.0284	0.7399	0.9936
		C_{Co} = 25	0.0194	0.573	0.8904	0.0359	0.6628	0.9949
		C_{Co} = 100	0.0176	0.481	0.936	0.0327	0.578	0.9905
	Co	C_{Cr} = 1	0.0195	4.703	0.8488	0.0142	4.9061	0.9998
		C_{Cr} = 5	0.0179	4.520	0.9148	0.0095	4.8194	0.9994
		C_{Cr} = 10	0.0215	4.312	0.9808	0.0094	4.7078	0.9995
Ni–Co	Ni	C_{Co} = 10	0.0162	3.411	0.8325	0.0137	3.6007	0.9995
		C_{Co} = 25	0.0141	3.005	0.8569	0.0131	3.1149	0.9992
		C_{Co} = 100	0.0149	2.598	0.9046	0.0126	2.7964	0.9987
	Co	C_{Ni} = 10	0.0197	4.211	0.9752	0.0081	4.6538	0.9995
		C_{Ni} = 20	0.016	3.609	0.8671	0.0074	3.8315	0.9969
		C_{Ni} = 50	0.0164	3.302	0.8777	0.0067	3.6574	0.9956

Table 2 also shows the effect of the temperature on diffusion rates of different stages. The larger the temperature, the faster the metal ion diffused. This result can be attributed to the fact that when the temperature increases higher the metal ions support higher drive force, drive force exhibit diffusion resistance and increase the diffusion rate.

The kinetic studies of Cr(VI), Ni(II), and Co(II) in binary system are also studied using two kinetic models as in single system. The adsorption rate constants are listed in Table 3. The correlation coefficients (r^2) obtained for the pseudo-second-order kinetic model were greater for all metals. It can be concluded that the adsorption process from binary systems follows pseudo-second-order kinetics.

Table 4
Adsorption isotherm parameters for the adsorption of Cr(VI), Ni(II) and Co(II) on zeolite 13x at different temperatures

			Temperature (K)			
Metal ions	Adsorption isotherms parameters		293	298	303	313
Cr(VI)	Langmuir	Q^0 (mg/g)	1.9981	2.5827	3.1733	3.9289
		b (L/mg)	0.1668	0.1562	0.1413	0.1348
		R^2	0.9939	0.9921	0.99	0.9877
	Freundlich	K_F (mg/g)	0.2978	0.3571	0.3982	0.4686
		n	1.3537	1.2906	1.2413	1.2019
		R^2	0.9893	0.9869	0.9861	0.983
	D-R	q_e (mg/g)	0.812	0.9511	1.0389	1.1639
		K_m (mol^2/kJ^2)	7.56E-3	6.42E-3	5.83E-3	5.61E-3
		E (kJ/mol)	8.1325	8.825	9.2608	9.4407
		R^2	0.9885	0.9889	0.9843	0.9908
	Redlich–Peterson	K_{RP}	0.2779	0.3384	0.3885	0.4614
		α_{RP}	0.0208	0.0105	0.0142	0.0063
		β	2.3037	2.9992	2.7963	3.9107
		R^2	0.9961	0.9963	0.9915	0.9924
Ni(II)	Langmuir	Q^0 (mg/g)	4.8375	5.3364	5.7523	6.195
		b (L/mg)	0.3162	0.4367	0.46	0.6443
		R^2	0.9942	0.9958	0.9919	0.9952
	Freundlich	K_F (mg/g)	1.4985	1.8834	2.0323	2.4946
		n	2.4673	2.5176	2.4286	2.438
		R^2	0.9583	0.959	0.953	0.9753
	D–R	q_e (mg/g)	3.585	4.0109	4.2627	4.5911
		K_m (mol^2/kJ^2)	5.43E-3	4.92E-3	4.36E-3	4.25E-3
		E (kJ/mol)	9.5958	10.081	10.708	10.846
		R^2	0.9588	0.9462	0.9371	0.8908
	Redlich–Peterson	K_{RP}	1.2299	2.0513	2.2617	4.5741
		α_{RP}	0.15	0.3027	0.2878	0.8718
		β	1.2067	1.1032	1.1404	0.9175
		R^2	0.9979	0.9965	0.9927	0.9954
Co(II)	Langmuir	Q^0 (mg/g)	8.181	8.8491	9.5528	10.389
		b (L/mg)	0.1716	0.2529	0.3	0.4501
		R^2	0.9965	0.9862	0.9914	0.9957
	Freundlich	K_F (mg/g)	1.6196	2.1362	2.4606	3.2793
		n	1.9385	1.9856	1.9246	1.9165
		R^2	0.9933	0.9439	0.9726	0.9813
	D–R	q_e (mg/g)	5.1299	5.8179	6.1311	6.7512
		K_m (mol^2/kJ^2)	5.16E-3	4.65E-3	4.14E-3	3.95E-3
		E (kJ/mol)	9.8437	10.369	10.989	11.251
		R^2	0.9458	0.9554	0.9211	0.9154
	Redlich–Peterson	K_{RP}	1.3224	1.6969	2.6497	4.7867
		α_{RP}	0.1319	0.0593	0.2231	0.4827
		β	1.0752	1.5056	1.0984	0.9751
		R^2	0.9959	0.9957	0.9897	0.9946

3.5. Adsorption isotherms

The experimental equilibrium sorption data have been tested by the two-parameter models of Langmuir [37], Freundlich [38], Dubinin–Radushkevich (D–R) [39], and Redlich–Peterson [40]. The reported linearized equations of sorption models are given as follows:

$$\frac{C_e}{q_e} = \frac{1}{Q^0 b} + \frac{C_e}{Q^0} \tag{8}$$

$$\ln q_e = \ln K_F + \frac{1}{n} \ln C_e \tag{9}$$

$$\ln q_e = \ln K_m - \beta \varepsilon^2 \tag{10}$$

$$q_e = \frac{K_{RP} C_e}{1 + \alpha_{RP} C_e^{\beta}} \tag{11}$$

The linear regression lines obtained from Langmuir isotherm graphs of C_e/q_e against C_e, give highly significant regression coefficient values closer to unity (Table 4), and small relative standard error of the goodness-of-fit of the models than the other isotherm equations indicating that sorption data better fit the Langmuir isotherm model. The value of dimensionless parameter, R_L, is less than unity (Table 4), which manifest that the sorption is favored under the applied conditions. According to the Langmuir assumption, the maximum monolayer adsorption capacity for Cr(VI), Ni(II), and Co(II) are 3.929, 6.195, and 10.39 mg/g, respectively. Values of the adsorption capacity of other adsorbents from literature are given in Table 5 for comparison. It is clear from the table that the adsorption capacities of zeolite 13x for Cr(VI), Ni(II), and Co(II) are comparable with the other adsorbents [41–50].

The Langmuir, Freundlich, D–R, and Redlich–Peterson isotherm constants along with the correlation coefficients were listed in Table 4. As can be seen from Table 4, the Langmuir isotherm model gave the highest R^2 value, showing that the equilibrium data of Cr(VI), Ni(II), and Co(II) adsorbed by zeolite 13x were best represented by this model. The variation of the adsorption intensity (R_L) with different temperatures of the solution is shown in Table 4. The maximum R_L value is 0.5974, 0.1365, and 0.1890 mg/L. This parameter ($0 < R_L < 1$) indicates that the zeolite 13x was a suitable adsorbent for the adsorption of Cr(VI), Ni(II), and Co(II) from aqueous solution. The equilibrium data were also fitted to the linear Freundlich equation for the adsorption of Cr(VI), Ni(II), and Co(II) onto zeolite 13x. Linear plot of log q_e vs. log C_e was examined to obtain K_F and n values. From the plot, the K_F values were found to be increased with the temperature rising from 293 to 313 K. The n value above 1 indicated that the adsorption of Cr(VI), Ni(II), and Co(II) by zeolite 13x was favorable at studied conditions. R^2 value was found to be 0.9860, which means that the

Table 5
Comparison of adsorption capacity of zeolite 13x with other adsorbents for Cr(VI), Ni(II) and Co(II)

	Adsorbent	Q^0 (mg/g)	Reference
Cr(VI)	Chemically treated *Helianthus annuus*	7.264	[41]
	Coir pith	165	[42]
	Acrylic acid-grafted coir pith	196	
	Hydrous zirconium oxide	66	[43]
	CTAB-silica gelatin composite	20.82	[44]
Ni(II)	Arthrobacter viscosus biofilm supported on zeolite	28.37	[45]
	Multiwall carbon nanotube/iron oxide magnetic composites	9.18	[46]
	Natural kaolinite clay	0.9	[47]
	EDTA-chitosan	71	[48]
	DTPA-chitosan	53.1	
	Cross-linked chitosan-isatin Schiff's base resin	40.15	[49]
	Modified with tetrabutylammonium(TBA) bromide kaolinite	8.4	[50]
	Modified with tetrabutylammonium(TBA) bromide montmorillonite	19.7	
Co(II)	EDTA-chitosan	63	[48]
	DTPA-chitisan	49.1	
	Cross-linked chitosan-isatin Schiff's base resin	53.51	[49]
	Modified with tetrabutylammonium(TBA) bromide kaolinite	9.0	[50]
	Modified with tetrabutylammonium(TBA) bromide montmorillonite	22.3	
	Chitosan-coated perlite beads	66.66	[51]

Freundlich model is not able to adequately describe the relationship between the amount of sorbed Cr(VI), Ni(II), and Co(II).

3.6. Thermodynamic study

The equilibrium constant (K_d, L/g) for the adsorption of Cr(VI), Ni(II), and Co(II) on zeolite 13x was calculated at the temperature of 293, 298, 303, and 313 K using Eq. (12):

$$K_d = \frac{Q_e}{C_e} \tag{12}$$

Thermodynamic parameters, Gibbs free energy change (ΔG°), the enthalpy change (ΔH°), and the entropy change (ΔS°), were calculated using the following equations:

$$\ln K_d = \frac{\Delta S^\circ}{R} - \frac{\Delta H^\circ}{RT} \tag{13}$$

$$\Delta G^\circ = -RT \ln K_d \tag{14}$$

The values of ΔH° and ΔS° can be obtained from the slope and intercept of the plot of ln K_d vs. $1/T$ (Table 6).

The Gibbs free energy change (ΔG°) was calculated to be negative values for Cr(VI), Ni(II), and Co(II) adsorption, which indicated the feasibility of the process and spontaneous nature of the adsorption, in each of the temperatures studied. Moreover, the ΔG° values increased with an increase in temperature, indicating corroborate high affinity of the metal for the sorbent substrate [51]. The ΔH° parameter was found to be 19.55, 50.77, and 43.80 kJ/mol for Cr(VI), Ni(II), and Co(II) adsorption, respectively. The positive values of ΔH° further confirmed the endothermic nature of adsorption process. The heat of adsorption value indicates the chemisorption process [52]. Hence, the adsorption of Cr(VI), Ni(II), and Co(II) on zeolite 13x was chemical in nature. The positive values of ΔS° (75.18, 192.63, and 168.43 J/(mol K)) suggested that the degrees of freedom increased at the solid-liquid interface during the adsorption. During the adsorption process, the coordinated water molecules were displaced by metal cations, resulting in increased randomness in the adsorbent–adsorbate system [53,54].

Table 6
Thermodynamic parameters for the adsorption of Cr(VI), Ni(II) and Co(II) on zeolite 13x at different temperatures

Metal ions	Temperature (K)	ΔG° (kJ/mol)	ΔH° (kJ/mol)	ΔS° (J/(mol K))
Cr(VI)	293	−2.349	19.55	75.18
	298	−2.966		
	303	−3.353		
	313	−3.893		
Ni(II)	293	−5.407	50.77	192.63
	298	−6.606		
	303	−7.213		
	313	−8.873		
Co(II)	293	−5.519	43.80	168.43
	298	−6.774		
	303	−7.696		
	313	−9.429		

The thermodynamic parameters also provided the best correlation of the experimental data in the studies carried out by Suksabye and Thiravetyan [42] on adsorption of Cr(VI) ions onto chemically modified coir pith, by Nuhoglu and Malkoc [53] on biosorption of Ni(II) ions onto waste pomace of olive oil factory (WPOOF), and by Bhattacharyya and Gupta [49] on adsorption of Co(II) ions onto calcined TBA-kaolinite. The adsorption of Cu(II), Ni(II), and Cr(VI) ions by

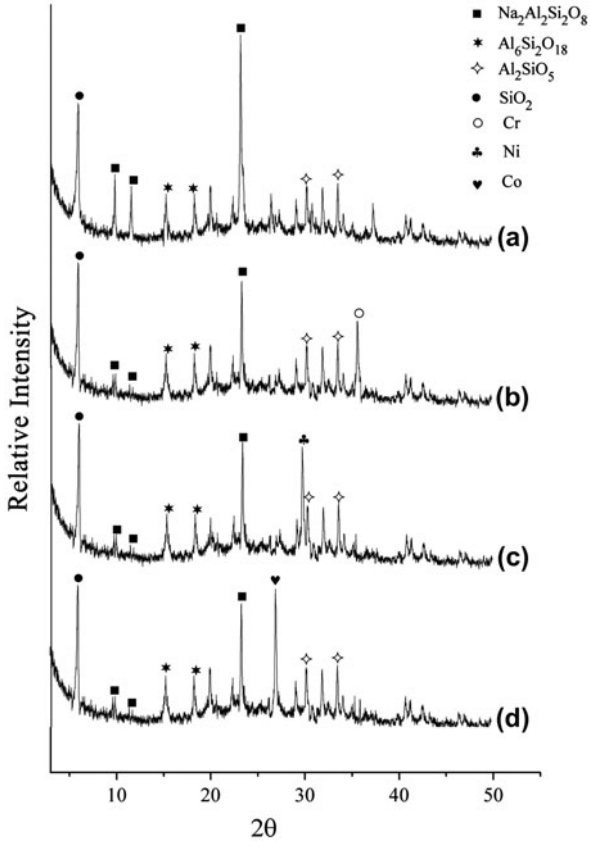

Fig. 5. XRD scans before adsorption (a) and adsorption of Cr(VI) (b), Ni(II) (c) and Co(II) (d).

modified oak sawdust in the study carried out by Argun et al. [54] also was demonstrated that the adsorption process was spontaneous and endothermic under natural conditions, in agreement with the thermodynamic parameters found in our study.

3.7. X-ray diffraction

XRD is an effective method for the investigation of the intercalation in zeolite 13x. Fig. 5 shows the XRD pattern of Cr(VI), Ni(II), and Co(II) supported on zeolite 13x. By comparing Fig. 4(a)–(d), one can see that the XRD peak position and intensities of SiO_2 ($2\theta = 6.11$), $Al_6Si_2O_{13}$ ($2\theta = 15.50$, $2\theta = 18.46$), and Al_2SiO_5 ($2\theta = 30.40$, $2\theta = 33.71$) are not shifted due to the characteristics of zeolite. But the intensity of the characteristic peak of $Na_2Al_2Si_2O_8$ ($2\theta = 10.01$, $2\theta = 11.76$, $2\theta = 23.40$) obviously weak, which indicated that metal ions adsorbed mainly in $Na_2Al_2Si_2O_8$. The parent zeolite 13x has surface area of around 500 m^2/g and micropore volume close to 0.5 cm^3/g, both typical values found for faujasites ($Na_2Al_2Si_2O_8$). The average pore width also did not change after adsorbtion Cr(VI), Ni (II), and Co(II), suggesting that the pore openings are mostly intact [32].

3.8. Desorption studies

Studying of desorption is helpful for exploring the possibility of recycling the adsorbents and recovery of metal resource. In this study, $CaCl_2$, NaOH, NaCl, HCl, and distilled water were used as eluents. The percentages of metal ions desorption for each eluent are shown in Fig. 6. It was obvious that HCl showed relatively good desorption results (58.57, 66.32, and 70.62%, respectively). However, $CaCl_2$, NaOH, NaCl, and distilled water were not efficient eluents for the desorption of Cr(VI), Ni(II), and Co(II) ions that had been adsorbed on the adsorbent surface. In the process of practical application, 0.1 M HCl solution can be considered to apply for the desorption of Cr(VI), Ni(II), and Co(II) from Cr(VI)–Ni(II)–Co(II)–zeolite 13x.

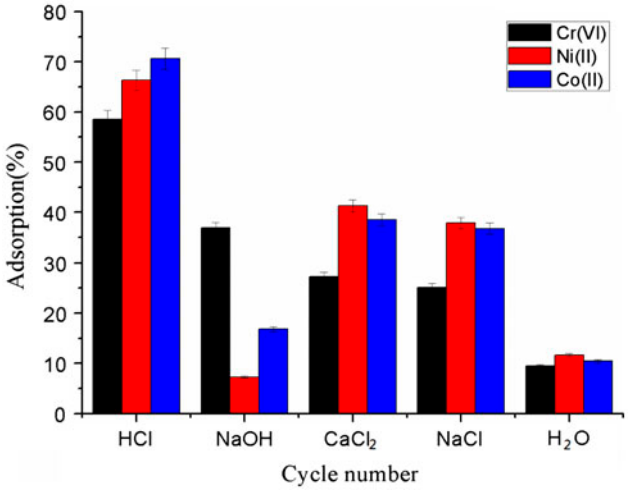

Fig. 6. Reusability of zeolite 13x by different desorbing agents with repeated sorption-desorption cycle.

4. Conclusions

The following conclusions can be inferred from this study.

(1) The removal rate of Cr(VI), Ni(II), and Co(II) on zeolite 13x increased with increasing pH value and temperature. The removal rate of metal ions decreased with an increase of initial concentration, while the maximum uptake increased with increasing the initial concentration.
(2) Kinetic data indicated that pseudo-second-order model was the best fit model; further, the uptake of sorbates was explained well by external diffusion and intra-particle diffusion model.
(3) The experimental data best fitted with the Langmuir isotherm. The monolayer adsorption capacity of Cr(VI), Ni(II), and Co(II) increased with increase in temperature and the maximum value was 3.929 mg/g, 6.195 mg/g, and 10.389 mg/g, respectively. The mean free energy (E) calculated from D–R isotherm commonly confirmed the chemical adsorption mechanism.
(4) Thermodynamic calculations showed that the Cr(VI), Ni(II), and Co(II) sorption process of zeolite 13x was endothermic and spontaneous. The positive value of ΔS^0 indicated that there was an increase in the randomness in the solid/solution interface system during the adsorption process.
(5) The desorption of Cr(VI), Ni(II), and Co(II) ions demonstrated that the best desorption performance was obtained by HCl, which meant that HCl can be regarded as one kind of eluents.

Nomenclature

$\gamma_{Al:Si}$ — the Al/Si ratio
R — the removal ratio (%)
q_e — the adsorption capacity at equilibrium (mg/g)
C_0 — the initial metal concentration (mg/L)
C_e — the equilibrium metal concentration (mg/L)

V — the solution volume (L)
M — the mass of the adsorbent (g)
q_t — the adsorption capacity at time t (mg/g)
k_f — the rate constant of pseudo-first-order sorption (1/min)
k_s — the corresponding kinetic constant (mg/(g min))
k_{ext} — the external diffusion rate constant (1/min)
k_{id} — the intra-particle diffusion rate constant (mg/g $s^{1/2}$)
I — the intercept (mg/g)
B — the Langmuir sorption equilibrium constant (L/mg)
Q^0 — the maximum monolayer uptake (mg/g)
K_F — the Freundlich adsorption constant ((mg/g) $(mg/L)^n$)
K_m — the D–R adsorption constant
ε — the D–R model constant
E — the mean free energy (kJ/mol)
K_{RP} — the Redlich–Peterson adsorption constant (l/g)
α_{RP} — the Redlich–Peterson model constant ($(L/mg)^{\beta}$)
β — the Redlich–Peterson adsorption constant
K_d — the equilibrium constant (L/g)
ΔG° — Gibbs free energy change
ΔH° — the enthalpy change (kJ/mol)
ΔS° — the entropy change (J/(mol K))
R — the universal gas constant (8.314 J/(mol K))
T — the absolute temperature (K)

References

[1] H.C. Ge, X.H. Fan, Adsorption of Pb^{2+} and Cd^{2+} onto a novel activated carbon-chitosan complex, Chem. Eng. Technol. 34 (2011) 1745–1752.
[2] H.B. Zhang, Z.F. Tong, T.Y. Wei, Y.K. Tang, Removal characteristics of Zn(II) from aqueous solution by alkaline Ca-bentonite, Desalination 276 (2012) 103–108.
[3] B. Shah, C. Mistry, A. Shah, Seizure modeling of Pb(II) and Cd(II) from aqueous solution by chemically modified sugarcane bagasse fly ash: Isotherms, kinetics, and column study, Environ. Sci. Pollut. Res. 20 (2012) 2193–2209.
[4] K.A. Shroff, V.K. Vaidya, Kinetics and equilibrium studies on biosorption of nickel from aqueous solution by dead fungal biomass of *Mucor hiemalis*, Chem. Eng. J. 171 (2011) 1234–1245.
[5] S. Durmaz-Sam, N.A. Sayar, A. Topal-Sarikaya, A.A. Sayar, Biosorption of Ni(II) by *Schizosaccharomyces pombe*: Kinetic and thermodynamic studies, Bioprocess Biosyst. Eng. 34 (2011) 997–1005.
[6] E. Repo, J.K. Warchol, T.A. Kurniawan, M.E.T. Sillanpää, Adsorption of Co(II) and Ni(II) by EDTA- and/or DTPA-modified chitosan: Kinetic and equilibrium modeling, Chem. Eng. J. 161 (2010) 73–82.
[7] M. Bansal, U. Garg, D. Singh, V.K. Garg, Removal of Cr(VI) from aqueous solutions using pre-consumer processing agricultural waste: A case study of rice husk, J. Hazard. Mater. 162 (2009) 312–320.
[8] F. Gode, E.D. Atalay, E. Pehlivan, Removal of Cr(VI) from aqueous solutions using modified red pine sawdust, J. Hazard. Mater. 152 (2008) 1201–1207.
[9] A. Ahmadpour, M. Tahmasbi, T.R. Bastami, J.A. Besharati, Rapid removal of cobalt ion from aqueous solutions by almond green hull, J. Hazard. Mater. 166 (2009) 925–930.
[10] K. Vijayaraghavan, T.V.N. Padmesh, K. Palanivelu, M. Velan, Biosorption of nickel(II) ions onto *Sargassum wightii*: Application of two-parameter and three-parameter isotherm models, J. Hazard. Mater. 133 (2006) 304–308.
[11] K. Anupam, S. Dutta, C. Bhattacharjee, S. Datta, Adsorptive removal of chromium(VI) from aqueous solution over powdered activated carbon: Optimisation through response surface methodology, Chem. Eng. J. 173 (2011) 135–143.
[12] W. Qiu, Y. Zheng, Removal of lead, copper, nickel, cobalt, and zinc from water by a cancrinite-type zeolite synthesized from fly ash, Chem. Eng. J. 145 (2009) 483–488.
[13] M. Sprynskyy, B. Buszewski, A.P. Terzyk, J. Namieśnik, Study of the selection mechanism of heavy metal (Pb^{2+}, Cu^{2+}, Ni^{2+}, and Cd^{2+}) adsorption on clinoptilolite, J. Colloid Interface Sci. 304 (2006) 21–28.
[14] M.G.A. Vieira, A.F.A. Neto, M.L. Gimenes, M.G.C. da Silva, Sorption kinetics and equilibrium for the removal of nickel ions from aqueous phase on calcined Bofe bentonite clay, J. Hazard. Mater. 177 (2010) 362–371.
[15] D.M. Manohar, B.F. Noeline, T.S. Anirudhan, Adsorption performance of Al-pillared bentonite clay for the removal of cobalt(II) from aqueous phase, Appl. Clay Sci. 31 (2006) 194–206.
[16] I. Smičiklas, S. Dimović, I. Plećaš, M. Mitrić, Removal of Co^{2+} from aqueous solutions by hydroxyapatite, Water Res. 40 (2010) 2267–2274.
[17] X.W. Zhao, G. Zhang, Q. Jia, C.J. Zhao, W.H. Zhou, W.J. Li, Adsorption of Cu(II), Pb(II), Co(II), Ni(II), and Cd(II) from aqueous solution by poly(aryl ether ketone) containing pendant carboxyl groups (PEK-L): Equilibrium, kinetics, and thermodynamics, Chem. Eng. J. 171 (2011) 152–158.
[18] E. Repo, T.A. Kurniawan, J.K. Warchol, M.E.T. Sillanpää, Removal of Co(II) and Ni(II) ions from contaminated water using silica gel functionalized with EDTA and/or DTPA as chelating agents, J. Hazard. Mater. 171 (2009) 1071–1080.
[19] M.V. Dinu, E.S. Dragan, Heavy metals adsorption on some iminodiacetate chelating resins as a function of the adsorption parameters, React. Funct. Polym. 68 (2008) 1346–1354.
[20] G.P.C. Rao, S. Satyaveni, A. Ramesh, K. Seshaiah, K.S.N. Murthy, N.V. Choudary, Sorption of cadmium and zinc from aqueous solutions by zeolite 4A, zeolite 13x and bentonite, J. Environ. Manage. 81 (2006) 265–272.
[21] F. Bai, H.W. Ma, Y.B. Wang, Adsorption capability of 13x zeolite molecular sieve to Hg^{2+} in water: An experimental study, Earth Sci. Front. 12 (2005) 165–170.
[22] D. Muraviev, R.K. Khamizov, N.A. Tikhonov, J.G. Morales, Clean ("Green") ion-exchange technologies.

4. High-Ca-selectivity ion-exchange material for self-sustaining decalcification of mineralized waters process, Ind. Eng. Chem. Res. 43 (2004) 1868–1874.
[23] M. Trgo, J. Perić, N.V. Medvidović, Investigations of different kinetic models for zinc ions uptake by a natural zeolitic tuff, J. Environ. Manage. 79 (2006) 298–304.
[24] C.H. Qin, R. Wang, W. Ma, Adsorption kinetic studies of calcium ions onto Ca-selective zeolite, Desalination 259 (2010) 156–160.
[25] A.E. Giannakas, M. Antonopoulou, Y. Deligiannakis, I. Konstantinou, Preparation, characterization of N–I co-doped TiO_2 and catalytic performance toward simultaneous Cr(VI) reduction and benzoic acid oxidation, Appl. Catal., B 140–141 (2013) 636–645.
[26] N. Wang, Y.Z. Xu, L.H. Zhu, X.T. Shen, H.Q Tang, Reconsideration to the deactivation of TiO_2 catalyst during simultaneous photocatalytic reduction of Cr(VI) and oxidation of salicylic acid, J. Photochem. Photobiol., A201 (2009)121–127.
[27] Q.L. Yang, Q.M. Lu, Z.F. Liu, S.P. Liu, G.C. Chen, H. Duan, D. Song, J. Wang, J. Liu, Resonance Rayleigh scattering spectra of ion-association nanoparticles of $[Co(4\text{-}[(5\text{-chloro-2-pyridyl}) \text{ azo}]\text{-}1,3\text{-diaminobenzene})_2]^{2+}$-sodium dodecyl benzene sulfonate system and its analytical application, Anal. Chim. Acta 632 (2009) 115–121.
[28] M. Kragović, A. Daković, Živko Sekulić, M. Trgo, M. Ugrina, J. Perić, G.D. Gatta, Removal of lead from aqueous solutions by using the natural and Fe(III)-modified zeolite, Appl. Surface Sci. 258 (2012) 3667–3673.
[29] H. Mekatel, S. Amokrane, A. Benturki, D. Nibou, Treatment of polluted aqueous solutions by Ni^{2+}, Pb^{2+}, Zn^{2+}, Cr^{+6},Cd^{+2} and Co^{+2} ions by ion exchange process using faujasite zeolite, Procedia Eng. 33 (2012) 52–57.
[30] C. Quintelas, V.B. da Silva, B. Silva, H. Figueiredo, T. Tavares, Optimization of production of extracellular polymeric substances by *Arthrobacter viscosus* and their interaction with a 13x zeolite for the biosorption of Cr(-VI), Environ. Technol. 32(14) (2011) 1541–1549.
[31] H. Figueiredo, B. Silva, C. Quintelas, M.M.M. Raposo, P. Parpot, A.M. Fonseca, A.E. Lewandowska, M.A. Bañares, I.C. Neves, T. Tavares, Immobilization of chromium complexes in zeolite Y obtained from biosorbents: Synthesis, characterization and catalytic behaviour, Appl. Catal., B 94(1–2) (2010) 1–7.
[32] M. Barkat, D. Nibou, S. Chegrouche, A. Mellah, Kinetics and thermodynamics studies of chromium(VI) ions adsorption onto activated carbon from aqueous solutions, Chem. Eng. Process. 48 (2009) 38–47.
[33] M. Ahmaruzzaman, S.L. Gayatri, Activated tea waste as a potential low-cost adsorbent for the removal of p-nitrophenol from wastewater, J. Chem. Eng. Data 55 (2010) 4614–4623.
[34] H. Spahn, E.U. Schlünder, The scale-up of activated carbon columns for water purification, based on results from batch tests—I, Chem. Eng. Sci. 30 (1975) 529–537.
[35] W.J. Weber, J.C. Morris, Kinetics of adsorption on carbon from solution, J. Sanit. Eng. Div. Am. Soc. Civ. Eng. 89(17) (1963) 31–60.
[36] V.L. Snoeyink, S.R. Summers, Adsorption of organic compounds, in: R.D. Letterman (Ed.), Water Supplies, 5th ed., McGraw-Hill Inc, New York, NY, 1999, pp. 13.11–13.83.
[37] I. Langmuir, The constitution and fundamental properties of solids and liquids. Part I. Solids, J. Am. Chem. Soc. 38 (1916) 2221–2295.
[38] H.M.F. Freundlich, Over the adsorption in solution, J. Phys. Chem. 57 (1906) 385–470.
[39] M.M. Dubinin, L.V. Radushkevich, Equation of the characteristic curve of activated charcoal, Chem. Zentr. 1(1) (1947) 875–889.
[40] Z. Aksu, Determination of the equilibrium, kinetic and thermodynamic parameters of the batch biosorption of nickel(II) ions onto *Chlorella vulgaris*, Process Biochem. 38 (2002) 89–99.
[41] M. Jain, V.K. Garg, K. Kadirvelu, Investigation of Cr(VI) adsorption onto chemically treated *Helianthus annuus*: Optimization using response surface methodology, Bioresour. Technol. 102 (2011) 600–605.
[42] P. Suksabye, P. Thiravetyan, Cr(VI) adsorption from electroplating plating wastewater by chemically modified coir pith, J. Environ. Manage. 102 (2012) 1–8.
[43] L.A. Rodrigues, L.J. Maschio, R.E. da Silva, M.L.C.P. da Silva, Adsorption of Cr(VI) from aqueous solution by hydrous zirconium oxide, J. Hazard. Mater. 173 (2010) 630–636.
[44] F. Venditti, F. Cuomo, A. Ceglie, L. Ambrosone, F. Lopez, Effects of sulfate ions and slightly acidic pH conditions on Cr(VI) adsorption onto silica gelatin composite, J. Hazard. Mater. 173 (2010) 552–557.
[45] C. Quintelas, R. Pereira, E. Kaplan, T. Tavares, Removal of Ni(II) from aqueous solutions by an *Arthrobacter viscosus* biofilm supported on zeolite: from laboratory to pilot scale, Bioresour. Technol. 142 (2013) 368–374.
[46] C.J. Chen, J. Hu, D.D. Shao, J.X. Li, X.K. Wang, Adsorption behavior of multiwall carbon nanotube/iron oxide magnetic composites for Ni(II) and Sr(II), J. Hazard. Mater. 164 (2009) 923–928.
[47] M.Q. Jiang, X.Y. Jin, X.Q. Lu, Z.L. Chen, Adsorption of Pb(II), Cd(II), Ni(II) and Cu(II) onto natural kaolinite clay, Desalination 252 (2010) 33–39.
[48] M. Monier, D.M. Ayad, Y. Wei, A.A. Sarhan, Adsorption of Cu(II), Co(II), and Ni(II) ions by modified magnetic chitosan chelating resin, J. Hazard. Mater. 177 (2010) 962–970.
[49] K.G. Bhattacharyya, S.S. Gupta, Calcined tetrabutylammonium kaolinite and montmorillonite and adsorption of Fe(II), Co(II) and Ni(II) from solution, Appl. Clay Sci. 46 (2009) 216–221.
[50] K. Swayampakula, V.M. Boddu, S.K. Nadavala, K. Abburi, Competitive adsorption of Cu(II), Co(II) and Ni(II) from their binary and tertiary aqueous solutions using chitosan-coated perlite beads as biosorbent, J. Hazard. Mater. 170 (2009) 680–689.
[51] M. López-Mesas, E.R. Navarrete, F. Carrillo, C. Palet, Bioseparation of Pb(II) and Cd(II) from aqueous solution using cork waste biomass. Modeling and optimization of the parameters of the biosorption step, Chem. Eng. J. 174 (2011) 9–17.
[52] B.A. Shah, A.V. Shah, R.R. Singh, N.B. Patel, Sorptive removal of nickel onto weathered basaltic andesite

products: kinetics and isotherms, J. Environ. Sci. Health. Part A Environ. Sci. Health 44 (2009) 880–895.
[53] Y. Nuhoglu, E. Malkoc, Thermodynamic and kinetic studies for environmentaly friendly Ni(II) biosorption using waste pomace of olive oil factory, Bioresour. Technol. 100 (2009) 2375–2380.
[54] M.E. Argun, S. Dursun, C. Ozdemir, M. Karatas, Heavy metal adsorption by modified oak sawdust: Thermodynamics and kinetics, J. Hazard. Mater. 141 (2007) 77–85.